 doi:10.20944/preprints202211.0084.v1

*Article*

# Heavy Ion Beam Probing Diagnostics on the TUMAN-3M Tokamak for Study Plasma Potential and Electric Fields in New Operational Regimes

**Leonid Askinazi*, Gulnara Abdullina, Alexander Belokurov, Vladimir Kornev, Sergei Lebedev, Dmitri Razumenko, Dmitri Shergin, Alexander Smirnov, Alexander Tukachinsky and Nikolai Zhubr**

* Correspondence: Institute, 194021, St.Petersburg, Russia, leonid.askinazi@mail.ioffe.ru (L.A.), abdullina@mail.ioffe.ru (G.A.), belokurov@mail.ioffe.ru (A.B.), vladimir.kornev@mail.ioffe.ru (V.K.), sergei.lebedev@mail.ioffe.ru (S.L.), d.razumenko@mail.ioffe.ru (D.R.), shergin994dima@gmail.com (D.S.), aismirnov@yahoo.com (A.S.), A.Tukachinsky@mail.ioffe.ru (A.T.), n.a.zhubr@mail.ioffe.ru (N.Z.)
* Correspondence: leonid.askinazi@mail.ioffe.ru

**Abstract:** Heavy Ion Beam Probing (HIBP) diagnostic is a powerful tool for electric field studies in hot dense plasma of modern day toroidal magnetic confinement devices. On the TUMAN-3M tokamak, the HIBP have been used in regimes with improved plasma confinement to clear up the role of radial electric field in the transition to good confinement regimes. Recently, a modernization of the TUMAN-3M HIBP diagnostics was performed aiming to reconfigure it for a work with a reversed plasma current direction and improvement of overall stability of the diagnostic. The results of first measurements of plasma potential in co-NBI scenario are reported and discussed.

**Keywords:** tokamak; plasma potential; radial electric field; L-H transition; Heavy Ion Beam Probing; Neutral Beam Injection

## 1. Introduction

Diagnostics of hot dense plasma in magnetic confinement fusion devices using the HIBP [1] provides important information about the dynamics of the electric potential, electric field, plasma density and poloidal magnetic field, as well as their fluctuations, in a wide range of spatial localizations, from the periphery to the central region, and discharge scenarios [2]. In many cases, this information is unique, since HIBP is the only technique that allows direct measurements of the potential and electric field in the hot plasma region. This diagnostics is not frequently used on torodal magnetic confinement devices due to a substantial technical complexity of its realization. A rare example of very interesting results and Alfven waves (AW) and GAM physics obtained using HIBP is experiments on the TJ-II stellarator and T-10 tokamak performed by Melnikov et al [3]. Observation using the HIBP of a specific type of electric field pulsation were reported from CHS stellarator [4]. On LHD stallarator, the HIBP was used successfully for the investigation of the geodesic acoustic mode (GAM) induced by the energetic particles [5, 6]. A detailed study of interplay between the GAM and the turbulence was performed on JFT-2M tokamak [7].

The TUMAN-3M tokamak [8] has been operating for many years the HIBP diagnostic, which was used to study the dynamics of the radial electric field in different operating modes of the tokamak. With the help of this diagnostic, the role of the radial electric field in switching the modes of high and low confinement (the so-called L-H and H-L transitions) [9] was revealed in ohmically heated plasma, oscillations of the geodesic acoustic mode (GAM) [10] were found, the dynamics of the electric field during the L-H transition was studied in a scenario when this transition was initiated by the NBI in the opposite direction to the plasma current, so-called counter-NBI [11]. Recently, the TUMAN-3M tokamak has been operating mainly in the mode of injection of a heating beam in co-direction with the plasma current (co-NBI setup), since in such a configuration the confinement

Preprints (www.preprints.org) | NOT PEER-REVIEWED | Posted: 4 November 2022 doi:10.20944/preprints202211.0084.v1

of fast ions, and hence the efficiency of plasma heating, is noticeably higher. On the other hand, in this mode, the generation of a radial electric field occurs under the action of, at least, two mechanisms that cause a perturbation of the radial field $E_r$ of different signs: negative $E_r$ is generated due to the loss of fast ions, whereas positive $E_r$ arises due to the transfer of angular momentum to the plasma from the confined fast ions. These mechanisms act in different parts of the plasma cross section, and their relative efficiency depends on the parameters of the plasma (electron density and temperature) and the heating beam (energy, current, injection geometry). The use of HIBP can provide important information on the generation mechanisms and dynamics of the radial electric field in this regime.

The principles of HIBP are based on the injection into the plasma of a beam of accelerated ions with energy and mass; this provides a sufficiently large Larmor radius of the injected ions in comparison with the plasma dimensions: $r_L = (2mW)^{0.5}/qB > a$, where m, W, q are the mass, energy, and ion charge, B and a are the toroidal magnetic field and the minor radius of the plasma. For the parameters of the TUMAN-3M tokamak ($B < 1T$, $a = 25cm$), potassium, sodium and, in some cases, cesium ions with energies up to 100 keV are used. As a result of collisions with plasma electrons, ions with the double charge (secondary ions) are formed, the trajectories of which are separated from the trajectories of primary ions at the ionization point, since they have a different (smaller) radius of curvature in the magnetic field. The detector located outside the plasma receives secondary ions formed in some region localized in space along the trajectory of primary particles. From the characteristics of the secondary ion beam (energy, beam intensity), one can determine the plasma potential and density locally at the secondary ionization point, thus obtaining information about the evolution of the radial electric field. The displacement of the secondary beam in the toroidal direction can be related to the magnitude and distribution of the poloidal magnetic field.

The next section briefly describes the composition of the HIBP diagnostic complex at the TUMAN-3M tokamak and algorithm of primary and secondary ions trajectories simulations is presented. Further, the upgrade of the diagnostic complex HIBP is considered, aimed at improving the reliability of the diagnostics, increasing the collected information and reproducibility of measurements. To this end, implemented:

- Autonomous isolated power supply system for thermoionic source heating
- control system for primary beam angle of entry and position
- Primary beam profile control system
- Two-point detection system for secondary beam

## 2. Heavy ion beam probing diagnostic at the TUMAN-3M tokamak

The layout of the HIBP diagnostic on the TUMAN-3M tokamak is shown in Fig. 1. Diagnostic complex consists of the following main parts: linear accelerator of primary ions (2), primary beam ion duct (17) with two sets of steering plates that change the direction of beam propagation in the poloidal and toroidal directions (two pairs of plates in each direction), secondary ion duct with plates deflecting the secondary beam in the toroidal direction (18), and a secondary ion energy analyzer (3). LT-100 and LT-30 blocks from Glassman (currently XPPOWER, www.xppower.com) were used as high-voltage sources for powering the accelerator and analyzer. The accelerator and the analyzer have a common grounding point, galvanically connected to the ground of the mains, while the tokamak chamber is isolated and during the plasma discharge is under a "floating" potential, reaching values of 500 - 1000V due to the capacitive coupling between the chamber and the toroidal field coils.

The plasma potential $\Phi_{pl}$ at the ionization point of the primary beam is related to the energy of the primary $W_1$ and secondary $W_2$ beams by the following simple relationship:

Preprints (www.preprints.org) | NOT PEER-REVIEWED | Posted: 4 November 2022 doi:10.20944/preprints202211.0084.v1

$$\Phi_{pl} = \frac{W_2 - W_1}{\Delta q} \quad (1)$$

where Δq is the change in the charge state of the ion during ionization. Usually Δq = - e, (here e is the electron charge), because the probability of double and even more triple ionization is small. The measurement of the potential by this technique is based only on the energy conservation law and the potentiality of the electrostatic field and, and such is direct, because does not require additional assumptions and models of plasma behavior. At the same time, the determination of the spatial localization of the plasma region, in which the measurement is made using the HIBP, is possible only by calculating the trajectories of primary and secondary ions by solving the equations of motion. At a fixed position of the primary ion accelerator and the secondary ion energy analyzer, the location of the detection point in the poloidal plane is uniquely determined by the poloidal entry angle $\alpha_x$ and the energy of the primary ion $W_1$ of the given species. An example of detector grids formed by lines of equal entry angle and equal energy is shown in Fig. 2. Using detector grids calculated for different ions species, energies, magnetic configurations, etc., it is possible to adjust the HIBP layout for measurement in the required plasma region [9]. Generally speaking, since the Larmor radius depends on the energy $W_1$ and the ion mass m and the magnetic field strength B as $\propto (2mW_1)^{0.5}/B$, the shape of the detector grids is determined precisely by this combination of parameters, which, in principle, allows instead of relatively light ions ($Na^+$ , $K^+$) to use heavier ones ($Cs^+$), reducing their energy accordingly. However, from a technical point of view, such a replacement is not quite equivalent, since at lower accelerating voltages, the focusing properties of the ion optic system deteriorate and the beam current decreases. On the other hand, when using light ions for access to the central parts of the plasma, it would be necessary to raise the energy of probing ions much higher than 100 keV, which is the maximum possible in this setup of the HIBP on the TUMAN-3M tokamak. As a result, $Na^+$ or $K^+$ ions with an energy of 60 – 100 keV should be used for measurements at the periphery of a plasma column (when studying L–H transitions, peripheral MHD activity, edge modes – ELM, etc.), while $Cs^+$ ions with an energy of 25 - 55 keV - to study phenomena localized in the central part of the plasma, such as sawtooth oscillations, internal transport barriers, etc.

Preprints (www.preprints.org) | NOT PEER-REVIEWED | Posted: 4 November 2022 doi:10.20944/preprints202211.0084.v1

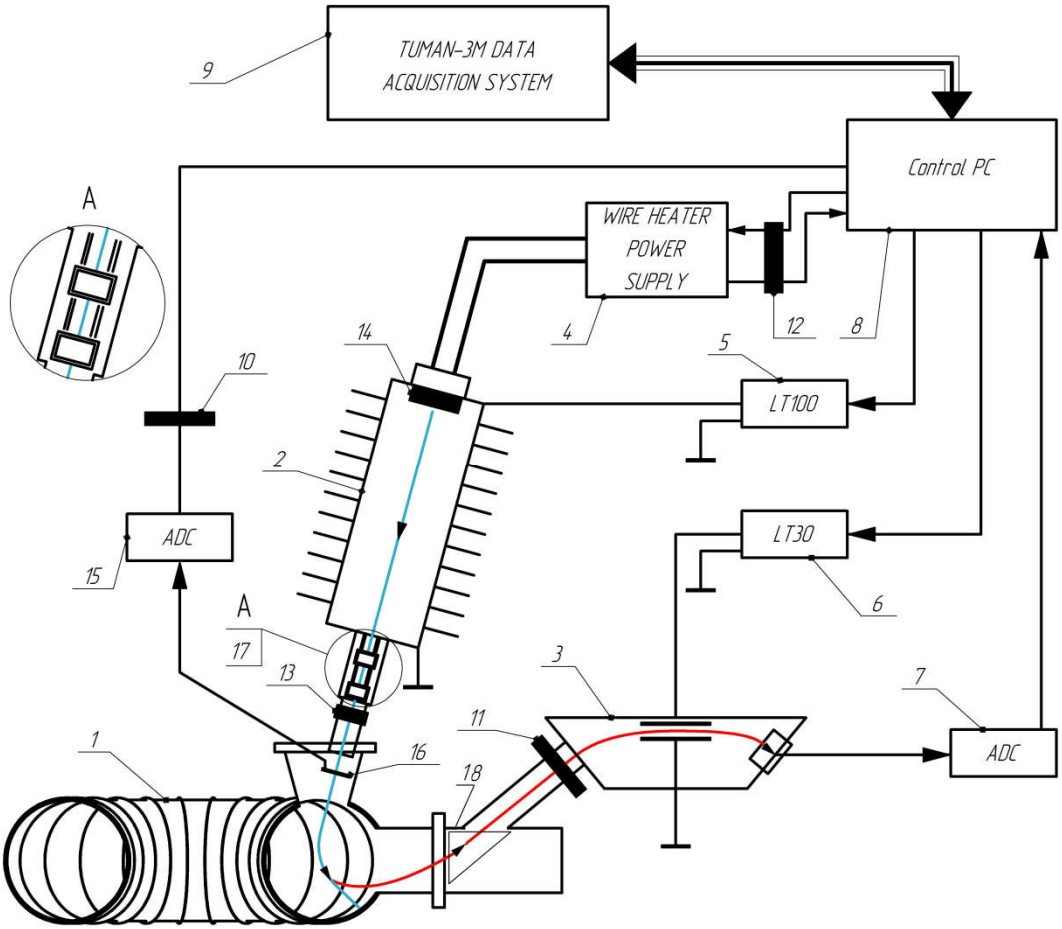


**Figure 1.** Layout of HIBP diagnostics at the TUMAN-3M tokamak. 1 - TUMAN-3M tokamak, 2 - Primary beam accelerator, 3 - Secondary ion energy analyzer, 4 - Autonomous isolated thermoionic source filament heater power supply, 5 - Accelerator high voltage power supply, 6 - Secondary ion energy analyzer high voltage power supply, 7 - DAC of secondary ion energy analyzer, 8 - Main control PC of HIBP, 9 - Data acquisition system of TUMAN-3M tokamak, 10-13- Galvanic isolation modules, 14 - Thermoion source of primary ions, 15 - DAC of primary beam wire array detector, 16 - Primary beam wire array detector, 17 - Primary beam steering plates box, 18 – Secondary beam steering box.

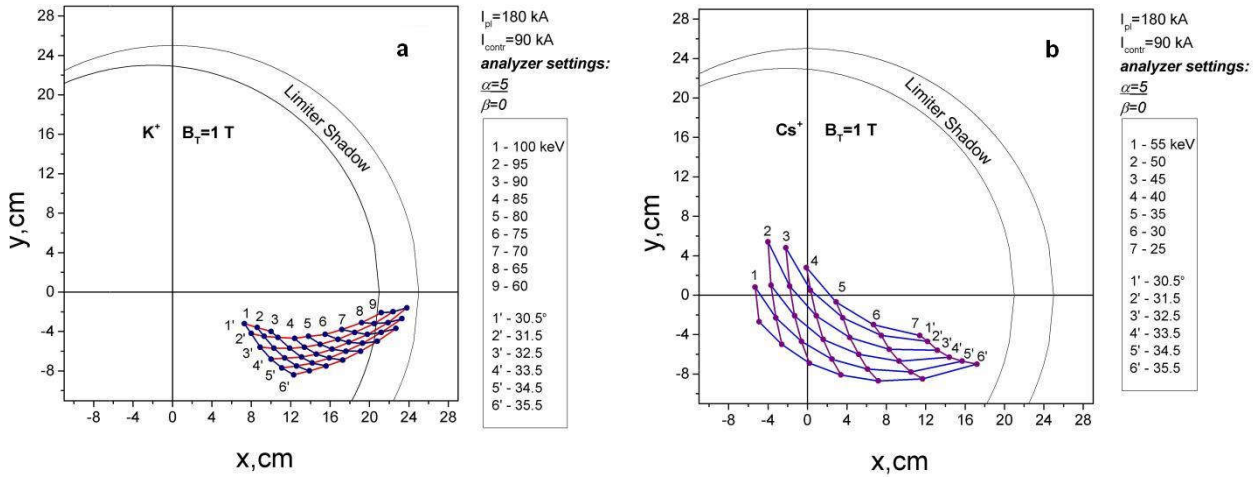


**Figure 2.** HIBP detection grids for $K^+$ (a) and $Cs^+$ (b) primary ions. Toroidal field $B_T$=1T, plasma current $I_p$=180 kA.

Preprints (www.preprints.org) | NOT PEER-REVIEWED | Posted: 4 November 2022 doi:10.20944/preprints202211.0084.v1

### 3. Autonomous isolated power supply system for the thermoionic source

The source of primary ions is a thermoionic source, which is a small fragment of remelted feldspar, heated by a filament with a current of about 12-18A to a temperature of about 500-1000 °C, and emitting singly charged $K^+$ or $Na^+$ ions, depending on the chemical composition of the feldspar. A feature of the diagnostic circuitry is that the thermoionic source must be under a high accelerating voltage, which requires the use of a controllable filament current source decoupled from the mains' ground. The previously used filament current source fed through an isolation transformer was unreliable and prone to breakdowns, which led to high voltage breakdowns and diagnostic failures. In the course of modernization, it was replaced by a specially designed autonomous fully isolated power supply powered by a lead battery with a voltage of 12 V and a capacity of 60 Ah, which makes it possible to carry out experiments for up to two days without recharging the battery. The source has an adjustable DC-DC converter, which makes it possible to control the filament current and, thus, to regulate the current of the primary HIBP beam. The source is enclosed in a metal equipotential shield electrically connected to the high voltage end of the primary ion accelerator and fixed on high-voltage insulators. To control the source, two optical light guide lines utilizing PWM technique with a length of about 20 m are used, connecting the HIBP located at the tokamak and the operator's workplace in the control room of the tokamak, and allowing remote control and measurement of the filament current. As a result of this modernization, it was possible to completely eliminate high-voltage breakdowns in the heating and accelerating circuits. The total primary beam current is measured using a Faraday cup inserted into the primary beam propagation channel with the help of a remotely controlled electromagnet, while primary current density profile is registered a 2D wire detector, see below.

### 4. Control system of the primary beam

As noted above, HIBP is a direct method for the plasma potential measurements, since it does not require any a priori assumptions and models of the interaction between the plasma and the probing beam, except for the fundamental principles - the energy conservation low and the potentiality of the electrostatic field. At the same time, there are currently no experimental methods for determining the position of the potential measurement point. In order to find out exactly where the measurement of the potential (as well as other plasma parameters) was made using the HIBP, it is necessary to simulate the propagation of the primary and secondary beams taking into account the actual magnetic configuration of the plasma installation, i.e., to solve the equations of motion of the primary and secondary ions with appropriate initial conditions. For the equation of motion of primary ions, these are the magnitude and direction of the velocity vector at the point of entry into the plasma, and the position of this point. The value of the velocity is uniquely determined by the accelerating voltage and the ion mass of the primary beam. To control the direction of the velocity vector and the position of the entry point, steering plates are used with a voltage of the appropriate magnitude and sign applied to them. For independent control of the position of the point of entry into the plasma and the direction of the velocity vector, there are two pairs of such plates (deflecting capacitors) for each of the orthogonal (to each other and to the injector's axis) coordinates x and z. The module with deflecting capacitors is installed between the primary beam accelerator and the inlet duct of the tokamak (position 17 in Fig. 1). The transverse beam entry coordinate $\Delta_i$ (i =x, z) and the angle between the velocity vector and the injector axis $\alpha$i are related to the voltages $U^i_1$, $U^i_2$ on the deflecting capacitors by the matrix equation

$$\begin{matrix}\Delta_i \\ \alpha_i\end{matrix} = M^i * \begin{matrix}V_1^i \\ V_2^i\end{matrix} \quad (2)$$

Here $V^i_k$ is the voltage on the corresponding deflecting capacitor, normalized to the accelerating voltage W: $V^i_k = U^i_k/W$. Matrix elements $M^i_{11}$ and $M^i_{12}$ have the dimension

Preprints (www.preprints.org) | NOT PEER-REVIEWED | Posted: 4 November 2022 doi:10.20944/preprints202211.0084.v1

"centimeter", $M^{i}_{21}$ and $M^{i}_{22}$ - "radian" and are determined by the geometric dimensions and position of the deflecting capacitors. For two transverse directions relative to the axis of the injector these matrices are

$$M^{x} = \begin{matrix} 124.7 & 119.2 \\ 1.1 & 2 \end{matrix}; \quad M^{z} = \begin{matrix} 109.6 & 89.2 \\ 1.1 & 2 \end{matrix} \tag{3}$$

The matrices are nondegenerate, which allows for solving the equations for the voltages $U^{i}_{1}$, and $U^{i}_{2}$, this makes it possible to set voltages on the deflecting capacitors that are necessary to obtain the initial conditions for the trajectory of the primary beam which are necessary for measuring the plasma parameters using the HIBP at the pre-requested spatial point. Since the deflection angles and beam displacement are small, in practice the voltages on the deflecting capacitors rarely exceed 1 – 2 kV, which makes it possible to use relatively low-voltage remotely controlled volage sources. Of course, the calculation results strongly depend on the position of the primary beam accelerator and the secondary beam energy analyzer, which must be known in each particular experimental configuration. In particular, the coordinate and angle of entry discussed above are defined with respect to the axis of the injector, and in order to calculate the trajectories, they must be recalculated taking into account the position of this axis in space, which can be changed mechanically within certain limits when adjusting the diagnostic. The diagnostic control software module has a built-in steering voltage adjustment interface, which accepts the required values $\Delta_i$, $\alpha_i$ (i = x, z) as input parameters and sets the required voltages on the controlled high-voltage sources. It is worth noting that steering plates located closer to the vacuum vessel of the tokamak mostly affect the entrance angle, whereas another pair of plates located further away from the vacuum vessel affects the position of the entrance point stronger. This circumstance may be used for a quick rough readjustment of the diagnostic between the tokamak shots.

**5. Control system of the primary beam profile**

To ensure the locality of measurements of plasma parameters using HIBP, it is necessary to have the minimum possible width of the primary beam in the volume of secondary ionization (sample volume). The measurement of the cross section of the primary beam and its position on entry into the TUMAN-3M vacuum vessel is carried out using a two-coordinate wire detector installed in the inlet duct of the tokamak, see pos. 16 in Fig. 1. It comprises a set of 10 wires (6 x 4 wires, x-dimension: 30mm; z-dimension: 18mm) with a 6mm spacing between the wires. The X-axis denotes the direction along the wire detector in the poloidal plane; the Z axis is the toroidal direction. The beam passing through the detector creates a current on the wires. The wire current detection system, consisting of analog multiplexer and an ADC, interrogates the current of each of 10 channels (wires) and feeds it through the ADC and a galvanically isolated communication line to a computer. Next, the signal is processed and the shape and parameters of the beam are restored. The software developed for this task processes the signal from the wires and, using the least squares method, restores the coordinates of the beam center, its width, and the total current; in the reconstruction, we used the assumption that the beam has a Gaussian shape, i.e., current density is given by:

$$j(x,z) = \frac{I_0}{\pi\sigma_x\sigma_z} e^{-\frac{(x-x_0)^2}{2\sigma_x{}^2} - \frac{(z-z_0)^2}{2\sigma_z{}^2}}$$

where $X_0$, $Z_0$ are the coordinates of the beam center along the corresponding axes; $\sigma_x$, $\sigma_z$ – beam half-widths in the corresponding directions at the level $e^{-0.5}$; $I_0$ is the total beam current. A visualization function is also provided that displays the spatial distribution in two orthogonal cross-sections and as a 2-dimensional distribution of the current density in the beam (Fig. 3 (a)), which facilitates real-time tuning of the primary HIBP beam. The use of this system makes it possible to quickly adjust the position and width of the primary

Preprints (www.preprints.org) | NOT PEER-REVIEWED | Posted: 4 November 2022 doi:10.20944/preprints202211.0084.v1

beam on entry into the tokamak vessel. When studying plasma using HIBP, it is necessary to know exactly the size and position of the secondary ionization region; when implementing a two-point measurement scheme (in which the analyzer is equipped with a double set of entrance slits and detector modules, thus making it possible to measure plasma parameters in two close spatial regions), it is also necessary to know the relative position and degree of possible overlap of the two sample volumes. The change in the beam width with its propagation along the trajectory in a given magnetic field of the tokamak is determined by two factors: focusing with an electrostatic lens in the injector and beam deformation in the inhomogeneous magnetic field. As a result of numerical calculation of the beam propagation, an optimal, from the point of view of beam focusing in the measurement volume, is the beam size on the grid detector, which is slightly larger than the minimal possible, i.e., focusing of the primary beam should be carried out somewhat further than the grid detector, near the point of beam entry into the plasma. In this case, the influence of the focusing action of the inhomogeneous magnetic field of the tokamak turns out to be minimal, and a situation is reached in which the beam has a minimum width at the sample volume. The focusing of the primary beam is controlled by means of an electrostatic lens formed by the potential distribution along the accelerating tube just near the thermoionic source, see Fig. 3 (b).

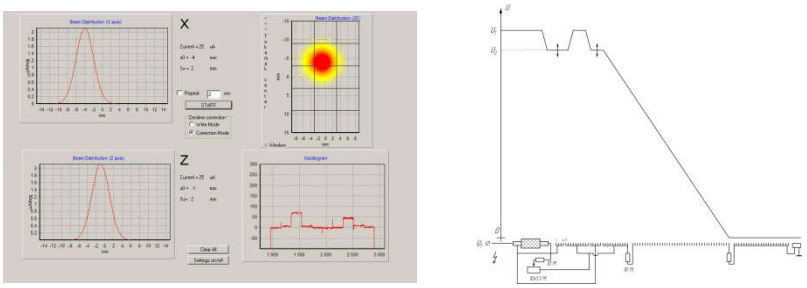

(a) (b)

**Figure 3. (a)** Program interface for primary beam current profile measurement and visualization; **(b)** Electric potential distribution along the accelerating tube of the primary beam. Beam propagates from left (thermoionic source) to right (tokamak TUMAN-3M vacuum vessel entrance).

In the potential distribution in the accelerator shown in Fig. 4, the voltage $U_1$ determines the energy of the primary ions $W_1=|e|U_1$, and the potential difference $U_2 - U_1$ forms an electrostatic lens; these voltages are set independently, which makes it possible to adjust focusing when the accelerating voltage changes. The focal length is calculated by the formula

$$f = \frac{4W_1}{\phi'_2 - \phi'_1}$$

where $\phi'_1$ and $\phi'_2$ are the potential gradients to the right and left of the lens. To check the correct operation of the primary ion acceleration system, the ion beam propagation in the injector was simulated using the SIMION numerical code [10]. The beam width was obtained from the modeling and measured experimentally using the grid detector described above. A comparison of the current profile of the $K^+$ beam with an energy of 60 keV, determined using a grid detector, and calculated using the SIMON code, is shown in Fig. 4. When modeling, it was assumed that the ions emitted by the thermoionic source have an angular spread of about $3^o$ with respect to the axis of the system. In the experiment, the accelerating voltage $U_1 = 60$ keV was fixed, and the change in the focal length of the lens was achieved by changing the "well" potential $U_2$. As expected, the beam width has a minimum at a certain value of the voltage in the “well” corresponding to focusing on the detector. When the focus voltage is changed, the focus shifts from the grid detector in one direction or another. It can be seen that the positions of the minima on the experimental and calculated dependences of the beam width on the detector on the voltage in the “well” coincide quite well, the difference in the “sharpness” of focusing is possibly

Preprints (www.preprints.org) | NOT PEER-REVIEWED | Posted: 4 November 2022 doi:10.20944/preprints202211.0084.v1

due to incorrect consideration of the angular spread of the ions emitted by the thermoionic source when modeling.

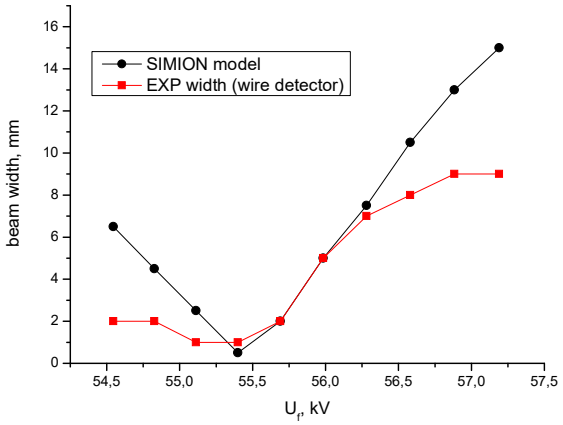


**Figure 4.** Comparison of the primary ion beam with measured by wire array detector (red squares) and modeled by SIMON [12] code (black circles), for different focusing voltages.

## 6. Measurement of the radial electric field in the TUMAN-3M tokamak using HIBP in the co-NBI heating scenario

Recently, we reported on influence of co-NBI on poloidal rotation velocity in TUMAN-3M plasma [13]. In this study the poloidal rotation velocity was measured using microwave Doppler backscattering. Previously [11], the evolution of the electric potential was studied in the TUMAN-3M tokamak in case of counter-NBI scenario, when the injection of a heating atomic beam is performed towards the plasma current. This scenario is unfavorable from the point of view of the efficiency of injection heating, since the confinement of fast ions is noticeably worse than in the case of injection of an atomic beam along the plasma current. Therefore, recently the tokamak power supply circuitry was reswitched for operating in the so-called co-NBI mode, when the directions of the plasma current and the velocity vector of the injected atoms coincide. The transition to this set up was implemented by changing the direction of the plasma current, since it was not possible to change the direction of atomic beam injection. As a result, both the direction of the poloidal magnetic field and the toroidal drift of the probing and secondary beams of the HIBP caused by it changed to the opposite. This required, in turn, a redesign on secondary ion beam guide connecting the secondary ion energy analyzer with the tokamak vessel. To this end, a custom connecting module was designed, manufactured and installed between the tokamak vessel and the analyzer, equipped with an interchangeable duct which allows for a relatively quick and simple switching the diagnostics to work with a different direction of the plasma current. Actually, the co-NBI scenario has recently become the standard mode of operation of the TUMAN-3M tokamak in both NBI and ohmic heating modes. Figure 5 presents the results of the first HIBP measurements of the dynamics of the electric potential in the regime with an L–H transition in this experimental set up. The measurements were carried out in a single point scheme, the sample volume was located near r = 10 cm. It is seen that L-H transition is accompanied by a noticeable drop in plasma potential $\Delta\Phi_{pl}$ ~ 100 V, manifesting a formation of negative radial electric field $E_r$ ~ -700 V/m in the region between the sample volume location and plasma edge. It must be taken into account that in the shot shown Fig.6, the L-H transition resulted from a joint action of co-NBI and a short (~5ms) pulse of working gas which was added simultaneously with the start of NBI pulse. In a similar shot with the same co-NBI power but without gas puffing no change in the confinement mode was observed. Contrary, in the absence of NBI, pulsed gas puffing easily triggers the transition in the TUMAN-3M tokamak, called in this case the ohmic L-H transition. So, one may conclude that confinement mode switching in

Preprints (www.preprints.org) | NOT PEER-REVIEWED | Posted: 4 November 2022 doi:10.20944/preprints202211.0084.v1

the shot in Fig. 5 is initiated not by the co-NBI but rather by the gas puffing pulse. NBI in this case, probably, somehow facilitates the transition, but, definitely, doesn't play a key role of a trigger.

It is interesting to note that it was observed earlier that ohmic L-H transition initiated by the gas puffing pulse in the TUMAN-3M also features a buildup of negative plasma potential up to -150 V [5], that is that is very close to potential perturbation measured in the experiments described here. On the other hand, in the L-H transition initiated by the counter-NBI heating, the plasma potential changed much stronger, up to 300-400 V below the ohmic L-mode level [11]. This comparison reflects different mechanisms responsible for the radial electric field formation in these scenarios. The accurate investigation of the $E_r$ using HIBP in two-point detection scheme, and comparison with other diagnostics' data is planned for the nearest future experiments.

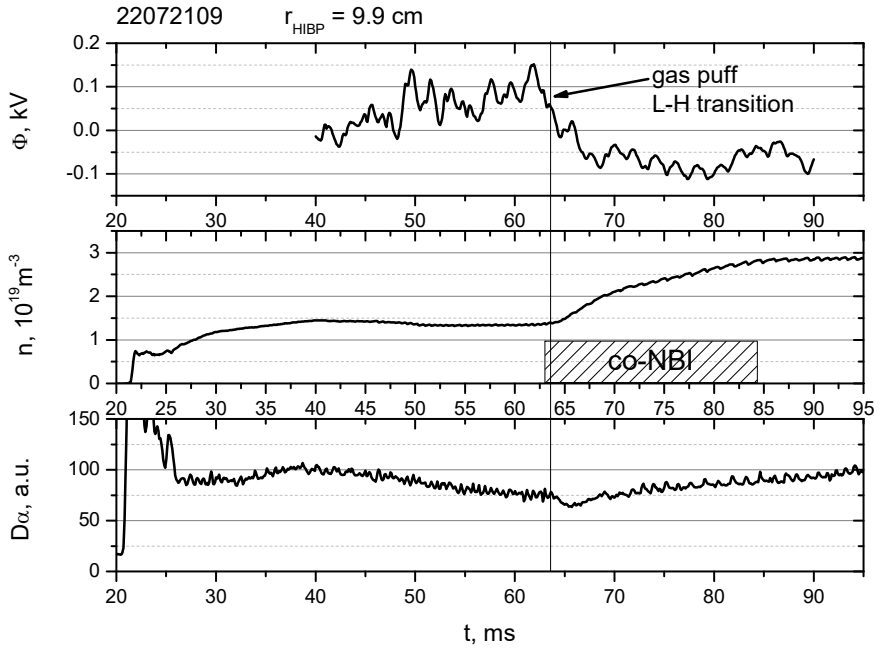


**Figure 5.** From top to bottom: Plasma potential evolution measured with HIBP, electron number density evolution, Da emission. L-H transition occurs at t=64ms, after the co-NBI pulse start.

## 7. Discussion

As a result of the modernizations and improvements made to the HIBP diagnostic of the TUMAN-3M tokamak, it is now possible to perform routinely the measurements of the plasma potential and radial electric field evolution in the plasma scenarios with a reversed plasma current direction, in which neutral heating beam is injected along the plasma current, first measurements performed in the discharge with L-H transition revealed some similarities with observations made earlier in ohmic H-mode regime and in the discharges with L-H transition triggered by counter-NBI. Namely, in all the scenarios the plasma potential becomes more negative after the transition, indicating the negative radial electric field build up at the plasma periphery, where H-mode transport barrier is being formed. The absolute value of the potential perturbation registered in the present experiments $\Delta\Phi \sim 150$V is close to the one observed in ohmic L-H transition scenario, and is much smaller than the one observed in counter-NBI triggered L-H transition. It may be a result of different mechanisms involved in radial electric field formation. For instance, the radial current caused by the fast particle losses is expected to be stronger in counter-NBI scenario due to the poor fast ion confinement, thus leading to the negative $E_r$ formation at the plasma periphery. In contrast, in co-NBI scenario, a positive $E_r$ should be generated close to the confinement region due to the direct momentum transfer from the

beam to the plasma. A detailed study of these and other possible acting mechanisms will be a subject of future investigation. The HIBP diagnostic will play a key role; its data will be compared against other diagnostics, such as Doppler spectroscopy, microwave Doppler reflectometry etc.

**Author Contributions:** Conceptualization, L.A. and A.B.; methodology, S.L.; software, N.Z.; validation, L.A., A.B. and A.S.; formal analysis, D.S.; investigation, A.T., V.K. and D.R.; resources, S.L., data curation, A.B.; writing—original draft preparation, L.A.; writing—review and editing, G.A.; supervision, L.A.; project administration, L.A.; funding acquisition, L.A. All authors have read and agreed to the published version of the manuscript

**Funding:** Operation and standard diagnostics on TUMAN-3M tokamak are supported by Ioffe Institute State contract 0040-2019-0023. HIBP modernization on TUMAN-3M tokamak is supported by Ioffe Institute State contract 0034-2021-0001. HIBP measurements on TUMAN-3M tokamak are supported by Russian Scientific Foundation project 22-12-00062.

**Data Availability Statement:** Not applicable.

**Conflicts of Interest:** The authors declare no conflict of interest.

**References**

1. Jobes, F.C. and Hickok, R.L. A direct measurement of plasma space potential. *Nuclear Fusion* **1970** *10* pp. 195-199 https://doi.org/10.1088/0029-5515/10/2/015
2. Askinazi, L.G., Chmyga, A.A., Dreval, N.B., et al. First HIBP Measurement of Plasma Potential During the H-Mode Transition on the TUMAN-3M Tokamak, In Proceedings of the ICPP 2002: 11th International Congress on Plasma Physics, Sidney, Australia, 2002, *AIP Conf. Proc.* **2002** *669* pp. 171-178
3. Melnikov, A.V., L.I. Krupnik, L.I., Eliseev, L.G., et al. Heavy ion beam probing – diagnostics to study potential and turbulence in toroidal plasmas, *Nucl. Fusion* **2017** *57* 072004
4. Fujisawa, A., Iguchi, H., Idei H., et al. Discovery of Electric Pulsation in a Toroidal Helical Plasma, *Phys. Rev. Lett*. **1998** *81* 2256–2259. DOI:https://doi.org/10.1103/PhysRevLett.81.2256
5. Ido, T., Shimizu, A., Nishiura, M., et al. Potential fluctuation associated with the energetic particle-induced geodesic acoustic mode in the Large Helical Device, *Nucl. Fusion* **2011** *51* 073046 (8pp) http://dx.doi.org/10.1088/0029-5515/51/7/073046
6. Ido, T., Osakabe, M., Shimizu, A., et al. Identification of the energetic-particle driven GAM in the LHD, *Nucl. Fusion* **2015** *55* 083024 (13pp), http://dx.doi.org/10.1088/0029-5515/55/8/083024
7. Kobayashi, T., Sasaki, M., Ido, T., et al Quantification of Turbulent Driving Forces for the Geodesic Acoustic Mode in the JFT-2M Tokamak *Phys. Rev. Lett*. **2018** *120* 045002 (4pp) https://doi.org/10.1103/PhysRevLett.120.045002 Vorobiev, G.M. et al. *Sov. J. Plasma Phys. (Fiz. Plasmy)* **1983**, *9*, 65
8. Askinazi, L.G., Kornev, V.A., Lebedev, S.V., et al. Heavy ion beam probe development for the plasma potential measurement on the TUMAN-3M tokamak *Rev. Sci. Instrum*. **2004** *75* pp. 3517-3519
9. Askinazi, L.G., Vildjunas, M.I., Zhubr, N.A. et al. Evolution of geodesic acoustic mode in ohmic H-mode in TUMAN-3M tokamak. *Tech. Phys. Lett.* **2012** *38* pp. 268–271, https://doi.org/10.1134/S1063785012030194.
10. Lebedev, SV., Askinazi, L.G., Chernyshev, F.V., et al. Counter-NBI assisted LH transition in low density plasmas in the TUMAN-3M. *Nucl. Fusion* **2009** *49* 085029, https://doi.org/10.1088/0029-5515/49/8/085029
11. SIMION software package: https://simion.com/
12. Yashin,A., Belokurov, A., Askinazi, L. et al, The Influence of Fast Particles on Plasma Rotation in the TUMAN-3M Tokamak, *Atoms* **2022**, *10*, pp. 106–120, https://doi.org/10.3390/atoms10040106